

TIME-TEMPERATURE HISTORIES OF BITUMINOUS COAL PARTICLES IN A DROP-TUBE REACTOR

Jonathan P. Mathews, Patrick G. Hatcher, Semih Eser, Peter M. Walsh^{*}, and Alan W. Scaroni
Fuel Science Program and Energy Institute, 211 CUL, The Pennsylvania State University,
University Park, PA 16802

^{*}Sandia National Laboratory, PO Box 969, Livermore, CA 94551

Keywords: drop-tube, particle size and shape.

Abstract

A device often used to simulate pulverized coal combustion conditions is the drop-tube reactor. It can adequately simulate residence times, heating rates, temperatures and flow conditions. Nevertheless, derived Arrhenius pre-exponential factors for devolatilization studies can span several orders of magnitude (1), probable due to difficulties in repeating time-temperature histories for different coals (2). CFD modeling of a simple drop-tube reactor incorporating coal particles as a second phase permitted time-temperature histories to be obtained for narrow size cuts for two bituminous vitrinites. Despite a narrow particle size distribution and the rank of the vitrinites being the same, significant differences were obtained in the time-temperature histories, among the size cut and between the vitrinite samples. Furthermore, the common and simplifying assumption of spherical particles for coal was found to underestimate the characteristic heating time by 22%, in comparison to the more reasonable "house brick" particle shape obtained from microscopic observations with video capture and computational analysis.

EXPERIMENTAL

The vitrain samples were collected from *Sigillaria* (a type of Lycopod) tree remains in the roofs of coal mines in the Upper Freeport (UF) and Lewiston-Stockton (LS) coal seams. The samples were first crushed in an adjustable plate mill to reduce the topsize to approximately 2mm, then comminuted in a Holmes 501 XLS pulverizer. Particle size separation was achieved by wet sieving. For shape analysis, polished pellets were prepared using a modified ASTM method. Size and shape analyses were performed using a digital image analysis system (IMAGIST, PGT, Princeton, NJ), in conjunction with a Nikon Microphot-FXA microscope and a workstation. The particle size distributions were determined with a Malvern laser light scattering instrument.

The drop-tube reactor consists of a single zone furnace operated at a maximum temperature of 1,400 °C, and is similar to previously described units (3). The reactor core is a high-purity alumina refractory tube, positioned vertically. The preheater temperature was 830 °C, and secondary nitrogen entered the top of the preheater from two inlets. The injector is water-cooled and also has a ceramic sheath for additional thermal protection. Coal is fed by an Acrison GMC-60 feeder at a rate of 0.33 g/min and is assumed to be entrained by the primary nitrogen. The tip of the injector is positioned level with the bottom of a mullite flow-straightener. Secondary nitrogen exited the flow-straightener with the primary nitrogen. The particle residence times are determined by the particle size, shape and the temperature and fluid-flow through the reactor.

Fluent™, a commercially available computational fluid dynamics (CFD) code, was used to model the gas and particulate flows within the furnace. The drop-tube was modeled in one dimension using symmetry around the centerline axis with a non-uniform grid consisting of 300 cells in length and 22 cells in radius. This grid covers the tip of the injector to the outlet of the ceramic reactor. The wall of the computational grid was arbitrarily split into eight sections and the temperature was assigned based on the average value (for that wall section) obtained experimentally using a suction pyrometer. The temperature of the wall was initially set to 50 °C above the average gas temperature for that section, this value being obtained from the difference between the reactor temperature (from the internal reactor thermocouple) and the gas temperature in the center of the hot zone of the reactor. Refinements were made to the wall temperatures until good agreement < 50 °C was obtained between the CFD and experimentally-determined temperature profile.

RESULTS

Particles were introduced into the CFD calculation as a second phase assuming perfectly spherical particles with densities of 1.4 g/cm³. Five particles were used to span the radius of the injector. The particles fall faster than the fluid; and hence are influenced by the particle diameter (mass is proportional to the radius³, but drag is proportional to the radius²), and changes in mass, volume and shape (which influences drag). A very narrow size cut of vitrinite (as measured by laser light scattering) was achieved by wet sieving. The difference between the D_v[0.1] and the D_v[0.9] (the volumetric weighted particle diameters such that 10 % and 90 % of the volume of the particles is in particles of greater diameters, respectively) was 66 and 53 μm for the Upper Freeport and Lewiston-Stockton vitrinites, respectively. The mean volumetric weighted particle diameters for the 200x400 US Standard Sieve cuts were 65 and 61 μm, for the Upper Freeport and Lewiston-Stockton vitrinites, respectively. Thus, a narrow distribution of time-temperature histories should be obtained for the vitrinites. However, this was not the case. The particle temperatures and residence times for the two extreme cases; the largest particle falling close to the centerline (particle 1) and the smallest particle falling closer to the wall (particle 5), are shown in Table 1. Cold flow experiments and initial CFD modeling indicated that the coal particles would fall in a narrow stream. Some radial growth in the coal stream occurs due to the expansion of the cold primary

nitrogen. However, under rapid-heating conditions, the coal particles fell as a cloud, presumably because of the "jet release" phenomenon (4) altering the particle trajectory. To better represent the particle trajectories a slight axial velocity was imposed on the particles. Particle 5 temperatures are higher at all sampling locations due to the closer proximity of the hot reactor wall (higher local gas temperature). At the 33 cm sampling location (distance from the injector) all the particles are close to the hot zone temperature (wall temperature of 1,400 °C), however, there are significant temperature differences between particles 1 and 5 at distances closer to the injector. The maximum observed difference in temperature between particles 1 and 5 is 320 K at the 23 cm sampling location for the UF case. These differences are, however, the extreme cases; visual observation indicated that the majority of the particles fell closer to the centerline than to the outer radius of the reactor. However, it is plausible that some of the collected particles can have quite different time-temperature histories despite the initially narrow particle size distribution and a drop-tube configuration designed for uniform time-temperature histories. Changes in particle size, mass and shape also influence the drag on the particle and hence the time-temperature history. The reactor temperature profile and morphological changes occurring to the LS 200x400 cut are shown in Figure 1. Significant swelling occurs for both vitrinites (2.5 and 1.8 times the mean particle diameters for the UF and LS vitrinites, respectively). This difference in swelling and a slight difference in mass loss resulted in slightly different time-temperature histories for the two vitrinites (Table 1).

Heat transfer and particle fluid-flow calculations often assume spherical particles. This is a reasonable assumption for both cases at the 33 cm location where the particles are almost exclusively cenospheric, but is a poor assumption for the initial vitrinite sample and the subsequent chars until the 23 cm sampling location (Figure 1). The silhouette of particles from the UF 200x400 cut is shown in Figure 2. Clearly there was a range of particle shapes; however, a sphere was not a good general shape representation. From >500 particle measurements the average aspect ratios are 1.7 for both vitrinite 200x400 cuts. This indicates that for a rectangular silhouette, the breadth is the length divided by 1.7. From SEM micrographs it was determined that to a first approximation, the depth could be assumed to be equal to the breadth. Thus, a square ended rectangular brick of length a and width and breadth of $a/1.7$ is a superior general shape descriptor than a sphere for these bituminous rank vitrinites. This shape descriptor has implications for both the particle residence time and the particle temperature. With a rectangular brick shape, the particle velocity is influenced by the particle orientation in the fluid. In comparison to a sphere of the same volume, the particle falling in the equilibrium position (oriented largest face down) has a similar coefficient of drag to that of a sphere (determined from terminal velocity measurements in an oil of known viscosity using square-ended bricks and spherical playdoh particles of the same mass). In contrast, the end-on orientation has a lower coefficient of drag and hence falls at a higher terminal velocity.

The non-spherical shape of coal particles has implications for commonly employed heating models. Deviation from spherical particles is reported to be responsible for the underestimation of radiative heating rate models (for 106-125 μm particles) by as much as 50% (5). In contrast, spherical carbon particles give a reasonable correlation between observed (optical pyrometry) and calculated heating rates. Combined convective and radiative models were also found to underestimate the heating rate for the same particles. Although there are uncertainties in many of the coal-related parameters and the effects of particle dispersion within the reactor in these calculations, the shape factors may also contribute significantly to the difference. Assuming that a vitrinite particle is adequately represented by a square ended rectangular brick, then equating the diameter of a sphere (d_p), of the same volume as the brick, to the length (a) yields equation 1.

$$\text{Vol} = \frac{a^3}{1.7^2} = \pi \frac{d_p^3}{6} \quad \text{or} \quad d_p = 0.87a \quad (1)$$

Sphericity (ϕ_s), the ratio of the surface area of a sphere to the surface area of the particle (of the same volume), yields equation 2, and substituting for d_p in equation 2 yields $\phi_s = 0.78$.

Incorporating this term in the commonly employed convective heating calculation yields equation 3, where Nu is the Nusselt number, λ is the thermal conductivity of the gas and T_g and T_p are the temperature of the gas and particle, respectively.

$$\phi_s = \frac{\pi d_p^2}{\left(\frac{2}{1.7^2} + \frac{4}{1.7}\right) a^2} \quad (2) \quad \frac{dQ}{dt} = \frac{\text{Nu}\lambda}{d_p} (T_g - T_p) \pi \frac{d_p^2}{\phi_s} \quad (3)$$

The sphericity term is in essence a corrective term for non-spherical particles. Incorporation of the energy gradient terms in equation 4 yields equation 5, where C_p is the specific heat of the particle, and ρ_p is the particle density.

$$\frac{\pi d_p^3}{6} \rho_p C_p \frac{dT_p}{dt} = \frac{\text{Nu}\lambda}{d_p} (T_g - T_p) \pi \frac{d_p^2}{\phi_s} \quad (4)$$

Rearranging equation 4 yields equation 5 and defining the characteristic heating time as τ yields equation 6.

$$\frac{dT_p}{dt} = \frac{6Nu\lambda}{d_p^2 \phi_s \rho_p C_p} (T_s - T_p) \quad (5)$$

$$\tau = \frac{d_p^2 \phi_s \rho_p C_p}{6Nu\lambda} \quad (6)$$

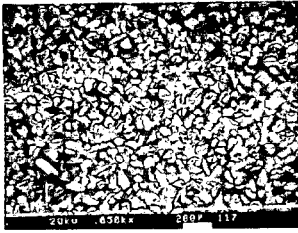
As $\phi_s=0.78$ and assuming $Nu=2$, the τ for the rectangular block is 22% greater than for the sphere. The $Nu=2$ assumption is valid for spheres in quiescent gas. A more accurate comparison would incorporate the influence of the square ended rectangular block geometry on the Nusselt number. Constant sphericity values of 0.73 for pulverized coal dusts and have been reported (6-7) based on microscopic and sieve analyses. A sphericity of 0.38 is also reported for fusain fibers (6), unfortunately the coal classification was not reported. A consistent shape factor (using surface areas as determined by liquid permeability and sieve sizes) has also been reported for various size cuts (11 fractions between 16 to 325 US mesh), although particle shape was found to be rank dependent (9). Aspect ratios of 1.39 to 1.55 have been determined for Pittsburgh seam coal dusts (less than 75 μm diameter) generated within the mine and by a variety of pulverizers (10). The sphericity factor reported here is consistent with some of the early work on coals (9).

CONCLUSIONS

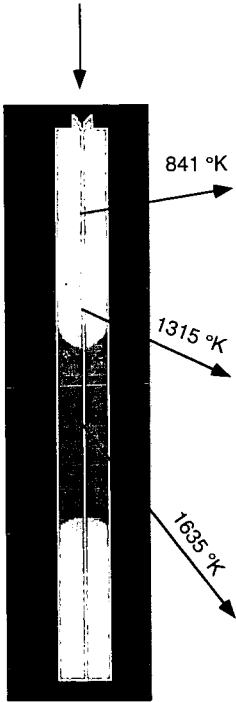
Significant variations were found in time-temperature histories between two narrow cuts of bituminous vitrinites in a drop-tube reactor. This was partially due to the influence of volatiles release, which alters the particle trajectory, but also to differences in mass loss and degree of swelling. The single particle shape descriptor of a sphere was significantly improved upon by using a square-ended rectangular brick. This shape can account for a 22% decrease in the characteristic heating time. The shape influences the drag and hence the particle residence-time.

REFERENCES

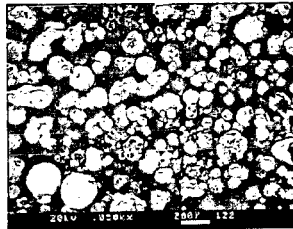
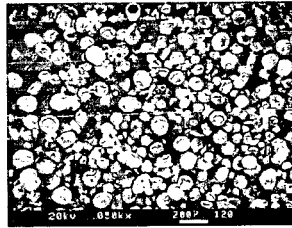
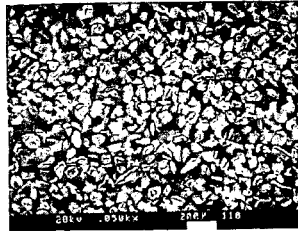
1. Smith, I. W., Nineteenth Symposium (Int) on Combustion, The Combustion Institute, Haifa, Israel, 1982, 1045.
2. Flaxman, R. J., and Hallett, L. H., *Fuel*, 1987, **66**, (5), 607.
3. Artos, V., and Scaroni, A. W., *Fuel*, 1993, **72**, (7), 927.
4. Grey, V. R., *Fuel*, 1988, **67**, (9), 1298.
5. Maloney, D. J., Monazam, E. R., Woodruff, S. D. and Lawson, L. O., *Combustion and Flame*, 1991, **84**, (1), 210.
6. Sakiadis, B. C., Fluid and Particle Mechanics, in Perry's Chemical Engineer's Handbook, Perry, R. G. and Green, D., 1984, McGraw, New York, Chapter 5.
7. Carman, P. C., *Trans. Inst. Chem. Eng. (London)*, 1937, **15**, 150.
8. Heywood, H., *I. Mech E.*, 1933, **125**, 383.
9. Austin, L. G., Gardner, R. P., and Walker, P. L., *Fuel*, 1963, **42**, (2), 319.
10. Li, J., Size shape and chemical characteristics of mining generated and laboratory-generated coal dusts, 1990, MS Thesis, The Pennsylvania State University.



SEM Micrograph of wet-sieved coal



Drop-tube Reactor Temperature Profile



Char Morphology

Figure 1. Fluid Temperature Profile and Char Morphology Changes for the Lewiston-Stockton Vitrinite

Table 1. Particle Residence Times and Temperatures at Various Sampling Locations

Distance from the injector / cm	Time / s			
	Particle 1(UF)	Particle 5(UF)	Particle 1(LS)	Particle 5(LS)
13	0.062	0.140	0.068	0.152
23	0.146	0.333	0.174	0.332
33	0.242	0.462	0.281	0.471
Temperature / K				
13	645	938	726	956
23	1090	1410	1230	1400
33	1600	1640	1630	1640

Table 2. Numbered Particle Silhouette Data

No.	Diam	Circ	E/R	A/R
1	27.3	3.21	0.37	2.70
2	102.8	2.87	0.43	2.33
3	61.9	1.74	0.77	1.30
4	58.0	7.83	0.19	5.26
5	105.2	1.83	0.62	1.61
6	61.8	1.78	0.85	1.18
7	70.6	1.52	0.90	1.11
8	69.3	1.74	0.64	1.56
9	91.3	4.90	0.28	3.57
10	57.5	2.08	0.65	1.54
11	85.5	2.94	0.50	2.00
12	89.5	2.11	0.55	1.82
13	16.1	2.83	0.43	2.33
14	87.0	1.42	0.82	1.22
15	56.8	2.07	0.64	1.56

Diam is the particle diameter in μm , Circ is the circularity, E/R the elongation ratio, A/R the aspect ratio.

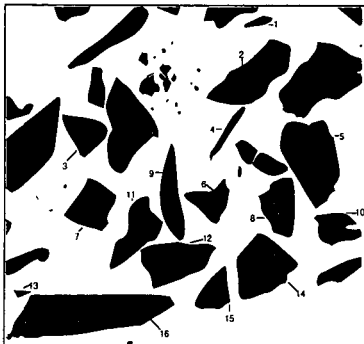


Figure 2. Silhouette of the 200x400 UF Vitrinite Cut